The synthetic peptide on titanium surface　enhances osteogenesis

합성펩타이드로 표면처리된 티타늄이 골형성에
미치는 영향

2017 년 2 월

서울대학교 대학원

치의학과 치주과학 전공

김 성 준

Abstract

The synthetic peptide on titanium surface enhances osteogenesis

Sung-Jun Kim

Program in Periodontology, Department of Dental Science

Graduate School, Seoul National University

Introduction

The oligopeptide including PHSRN and RGD sequence of fibronectin (F20) promoted cellular activity like adhesion, migration, proliferation and differentiation with various cells. In this study, the biologic effect to cellular activity of F20 on titanium (Ti) surface was investigated with the synthetic oligopeptide and evaluated as a biomolecule to improve the surface characteristics of dental implant.

Materials and Methods

The change of surface characteristics after applying synthetic F20 on machined and SLA Ti surface through adsorption was investigated with confocal laser scanning microscopy (CLSM) observation. The stromal cell line ST2 was used for cell source. The quality of coating was evaluated with fluorescence microscopy and confirmed with measuring of fluorescence intensity. SEM and CLSM observation for cell adhesion, cell migration

assembly kit for cell migration, Picogreen assay for cell proliferation, real time PCR and ALP activity assay for differentiation, and immunoblot and ALP staining and real time PCR for molecular mechanism was used for evaluation, respectively.

Results

The change of roughness with the coating of F20 was not remarkable. The surface characteristic of machined and SLA Ti was different after adsorption and observed with CLSM. Cell attachment was more enhanced on machined surface with F20 than SLA. The difference was more prominent in early stage after applying F20. Migration of ST2 cell was enhanced with F20 treatment in 6, 24 h. Cell proliferation and differentiation was stimulated with F20 apply. The extracellular signal-regulated kinase (Erk) signaling pathway was activated with F20 and confirmed with inhibitor U0126 apply.

Conclusions

From the findings of this study, F20 can be considered to promote osteoblast activity and stimulate differentiation through Erk signaling pathway. F20 can be a choice of biomaterials to improve surface modification of dental implant.

The synthetic peptide on titanium surface enhances osteogenesis

Sung-Jun Kim

Program in Periodontology, Department of Dental Science

Graduate School, Seoul National University

(Directed by Professor Young Ku, D.D.S., M.S.D., PhD.)

CONTENTS

I. INTRODUCTION

The surface modifications of the dental implant have been investigated to promote the better bone response during healing process after implant installation. The activities of osteoblasts such as spreading, adhesion, proliferation and differentiation would be influenced by the implant surface characteristics. [1, 2]

To achieve stronger and faster osseointegration, altering surface roughness and characteristics have been investigated with mechanical and chemical approach. Recently, many attempts to achieve better osseointegration through biomechanical methods have been studied using several biomolecules. [3, 4]

Cell adhesion is mediated by cell-surface receptors like integrins that are glycoproteins of cell membrane includes various kinds of heterodimer with specific ligand pairs: α1β1, α2β1, α3β1, α4β1, α5β1, α6β1, α8β1, αvβ1, αvβ3, αvβ6. [5,6] Integrins are important for cell migration in terms of that they directly mediate adhesion to the extracellular matrix, but also because they regulate intracellular signaling pathways that influence cytoskeletal formation and spreading. [7]

As a role of adhesion mediators that regulate the cytoskeleton, integrins are important in controlling various steps in the signaling pathways that regulate diverse processes like proliferation, differentiation, apoptosis, and cell migration. [8]

Among ligand pairs, a specific FN receptor, the α5β1 integrin, was reported to support a role for transducing cell responses to FN and considered to be required for osteoblast differentiation at very early stages in bone formation. [9] FN has a critical role in cellular activities like adhesion, proliferation and differentiation to bind with integrin. [6]

In many studies, a specific cell binding sequence, Arg-Gly-Asp (RGD), had shown the key role in binding with integrins that are crucial for cell-ECM interaction. [10-12]

Many previous studies have shown that FN has more importance in matrix organization than in reaction between bone matrix and cell ingredients in early stage of bone formation. [14]

The recombinant synthetic oligopeptide, a specific sequence DPHSRNSITGTNLTPGYTITVYAVTG-RGD, has shown the better bone formation response with enhancing cell adhesion and differentiation of osteoblast, and suggested the possibility as a useful bioactive material for bone graft. [15]

With a recombinant FN fragment including PHSRN and RGD sequence, cells showed the adherence to dominant distribution of integrin α5β1 and the enhanced spread of cell. [16]

Another previous study with peptide G3PHSRNG6RGDG showed the promoted cell attachment, spreading and Erk signaling pathway activation of human periodontal ligament (PDL) cell with the concentration of 10 μM. [17]

Some specific fibrin-binding oligopeptide sequence, designated as FF3 and FF5, can be considered to enhance cell attachment and mineralization of human osteoblast-like cells (HOS cells). [18] FF5 promoted bone formation in the defects of rabbit calvarias with deproteinized cancellous bovine bone particle at the early healing stage. [19]

Taken together, previous studies regarding the altered surface of biomaterials with oligopeptide derived from fibronectin had shown increased cellular activity of osteoblast. The strategy to promote the biocompatibility of biomaterials with the molecules is expressed as "biomimetic approach". [20]

The aim of this study was to evaluate the effect of fibronectin derived synthetic oligopeptide F20 on cellular adhesion, migration, proliferation, and

differentiation. To investigate the fundamental molecular mechanism of F20 on osteoblast, cell signaling pathway was also investigated.

II. MATERIALS AND METHODS

Cell culture

The stromal cell line ST2 was cultured in RPMI-1640 medium (Life Technologies, Carlsbad, CA, USA) as previously described. [21] The cell line was purchased from ATCC (Manassas, VA, USA). Cell culture media contains 10% fetal bovine serum (FBS; Life Technologies) and 1% penicillin/streptomycin (Life Technologies). Cells were seeded on discs at a density of 1×10^4 cells/cm^2 and incubated aerobically at 37℃ and 5% CO_2.

F20 oligopeptide synthesis

A synthetic F20 peptide was artificially produced through a custom peptide synthesis service (Peptron Inc., Daejeon, Korea) in the ordered sequence DPHSRNSITGTNLTPGYTITVYAVTGRGD, which has been previously reported [15]. Fluorescein isothiocyanate (FITC)-labeled F20 was also synthesized for the evaluation of the F20 coating on the disc surface after the adsorption process.

Surface treatment of Ti disc by the peptide

Ti specimens were prepared in disc shapes (120 mm in diameter and 1 mm in thickness) with machined or SLA surfaces (Osstem Implant Co., Ltd, Busan, Korea). Synthetic F20 was adsorbed onto the disc surfaces at 1 ng/ml concentration at 4°C for 24 h.

Surface roughness assessment

The average surface roughness (R_a) and surface topography of Ti discs were analyzed using a 3D confocal laser scanning microscope (CLSM; Carl Zeiss LSM700, Oberkochen, Germany). R_a values are presented as the mean ± SD of three independent experiments.

We used FITC-labeled F20 oligopeptide (FITC-F20) for the detection of adsorbed or detached F20 on the Ti discs. FITC-F20 (1 ng/ml) was adsorbed on the disc surfaces at 4°C, over 24 h, and then discs were moved to a new plate and observed for 7 d. F20 coating quality was directly and visually detected through fluorescence microscopy (Eclipse Ti Inverted Microscope; Nikon, Tokyo, Japan). Furthermore, conditioned media (100 µl) were harvested at specified time points (0, 1, 3, 5, 7 days) after the discs were moved to the new plate, and the fluorescence intensity was indirectly measured on a GloMax-Multi Detection System machine (Promega, Madison, WI, USA). Sampling was performed three times and values are presented as the mean ± SD of three independent measurements.

Cell attachment and morphology observation

Cell attachment was observed by scanning electron microscopy (SEM; HITACHI S-4700, Tokyo, Japan) and confocal laser scanning microscopy (CLSM; Carl Zeiss LSM700). Cells on the discs were harvested after 6 and 24 h for SEM observation, and after 12 and 24 h for CLSM. Cells were fixed in 4% formaldehyde. Fixed cells were coated with platinum (Pt) for SEM. For CLSM, fixed cells were stained with Hoechst 33342 (Invitrogen, Carlsbad, CA, USA) for detection of cell nuclei and Alexa Fluor 568 phalloidin (Invitrogen, Carlsbad, CA, USA) to visualize the cytoskeleton.

Cell migration assay

Oris Universe Cell Migration Assembly Kits (Platypus Technologies, WI, USA) were used for cell migration assays following the manufacturer's instructions. Oris 96-well plates were coated with F20 with concentrations of 0, 0.1, 1 and 10 ng/ml and dried overnight in a clean bench. The Oris stoppers were inserted each well before adding the cells. In each well, 1×10^4 ST2 cells suspended in DME was added and incubated for cell attachment for 3h at 37°C in 5% CO_2.

For cell growth arrest and anti-proliferation, mitomycin-C (MMC; Sigma-Aldrich) was used with the concentration of each well 30μg/ml for 2h before starting the assay. The stoppers were removed to allow cell migration to a 2 mm diameter in a centrally located detection zone for 3,6,24 h at 37°C in 5% $CO_2.$

After cells were fixed and stained with 10% NBF, 0.25% (w/v) toluidine blue at each point in time, samples were evaluated by light microscope (Olympus BH-2, Olympus Optical, Osaka, Japan) by taking a photograph of each sample using a digital camera (Olympus Optical, Osaka, Japan). An automated image analysis system (Tomoro Scope Eye 3.5 Image Analyzer, Techsan Digital Imaging, Seoul, Korea) was used for measurement of the migrated cell area comparing with 2 mm diameter centrally located detection zone.

Cell proliferation assay

The Picogreen assay was performed using the Quant-iT Picogreen assay kit (Invitrogen Ltd., Paisley, UK) at 1, 3, and 5 d after seeding cells on the discs. Cells were washed with phosphate-buffered saline (PBS) and lysed using TE buffer (10 mM Tris-HCl, 1 mM EDTA, pH 7.5). The DNA contents were determined by mixing 100 μl of Picogreen reagent and 100 μl of DNA sample. Samples were loaded in triplicate and fluorescence intensity was measured on a GloMax-Multi Detection System machine (Promega).

Fluorescence intensity was converted into DNA concentration with a DNA standard curve according to the manufacturer's instructions. Values are presented as the mean ± SD of three independent measurements.

Reverse-transcription PCR and quantitative real-time PCR

RNA was isolated from harvested cells using QIAzol lysis reagent (QIAGEN, Valencia, CA, USA). The Primescript RT reagent kit for reverse transcription was purchased from Takara Bio (Shiga, Japan). Quantitative real-time PCR was performed for the alkaline phosphatase (ALP) gene with a primer pair used previously [21, 22]. Quantitative real-time PCR was performed using Takara SYBR premix Ex Taq (Takara Bio) on an Applied Biosystems 7500 Real Time PCR system (Foster City, CA, USA). The PCR primer was synthesized by Integrated DNA Technology (IDT; Coralville, IA, USA). All experiments were run in triplicate, and the relative levels of mRNA were normalized to those of glyceraldehyde-3-phosphate dehydrogenase (GAPDH).

ALP activity assay

A standardized kit for the ALP activity assay was purchased from Takara Bio (Shiga, Japan). Cells were seeded on the discs and harvested at 1, 4, 8, and 11 d after seeding and washed with PBS, after which extraction/substrate/stop solutions were added according to the manufacturer's instructions. Absorbance was detected at 405 nm with a GloMax-Multi Detection System machine (Promega).

Immunoblot analysis

ST2 cells were serum starved for 16 h and treated with F20 (1 ng/ml). Cells were harvested at 10, 15, and 30 min after F20 treatment and washed with ice-cold PBS twice. Then, cellular proteins were isolated in a lysis buffer containing 50 mM HEPES (pH 7.5), 150 mM NaCl, 100 mM NaF, 1 mM DTT, 1 mM EDTA, 0.25% Na-deoxycholate, 0.25% CHAPS, 1% NP-40, and 10% glycerol supplemented with protease and phosphatase inhibitors, including Na_3VO_4. Immunoblot analysis was performed with anti-P44/42 MAPK (Erk1/2) and anti-phospho-P44/42 MAPK (Erk1/2) monoclonal antibodies purchased from Cell Signaling (Beverly, MA).

ALP histochemical staining

ST2 cells were cultured to 80% confluency and pretreated with U0126 (40 µM) for 1 h; then, they were incubated in the presence of F20 (1 ng/ml) for an additional 5 d. Cells were washed twice with PBS, and stained as described by the manufacturer. An ALP staining kit was purchased from Sigma-Aldrich (St. Louis, MO, USA).

Statistical analysis

All quantitative data are presented as the mean ± SD; each experiment was performed at least three times, and the results from one representative experiment are shown. Student t-test was used for the measurement of fluorescence intensity. Statistical analyses for cell proliferation assay, quantitative real-time PCR and ALP activity assay were performed using one-way analysis of variance (ANOVA) with Tukey's post hoc test. Post hoc analysis was used to detect pairs of groups with statistically significant differences. A statistical analysis for cell migration assay was performed using a Student's t –test with a 95% confidence interval.

Statistical analyses were performed using SPSS software (SPSS Statistics, Inc., Chicago, IL, USA). $p < 0.05$ was considered statistically significant for all tests.

III. RESULTS

Surface analysis of F20 coating Ti surfaces

CLSM was used to analyze the average roughness (R_a) and surface topography of each specimen. The R_a values of the machined surface and F20-coated machined surface were 0.24 ± 0.15 µm and 0.22 ± 0.12 µm, respectively. And those of the SLA surface and F20-coated SLA surface were 3.21 ± 0.23 µm and 3.12 ± 0.11 µm, respectively (Fig. 1A). F20-coated Ti disc surfaces showed similar surface roughness as uncoated surfaces ($p < 0.05$).

Evaluation of adsorption with F20 coating on the Ti surfaces

The evaluation of F20 coating was performed in both direct and indirect ways. Through the method of fluorescence microscopy, the quality of the F20 adsorption to the surface was assessed directly (Fig. 1B). And the fluorescence intensity of FITC-F20 of the culture media was detected indirectly to measure the detached F20 amount (Fig. 1C). At the temperature of 4°C for 24 hrs, the discs were submerged in FITC-F20 media; then replaced to a new plate and kept under the identical condition of culture. The pattern of adsorption showed the considerable difference between the two surfaces, machined and SLA. On the machined surface, the pattern of F20 coating seemed the homogenous layer and some part of that was slightly detached (a, Fig. 1B). Conversely, the irregular heterogeneous layer with peak and pit was observed on the SLA surface (b, Fig. 1B). This uneven and

irregular surface characteristic is also seen from Fig 1A. On SLA surface, F20 was placed primarily on the convex peak portions (b, Fig 1B).

Measuring the fluorescence level in the media after transferring the disc to the new plate showed the level of detachment of F20 from the surface. In the initially stage, the level of fluorescence intensity soared up and became slower in progress and finally showed flatter increase in final stage (Fig. 1C; a: machined, b: SLA). At day 1 on machined surface, the amount of detached F20 was shown prominent through the course of days. Meanwhile, the progress was different with the peak rate of day 3 on SLA surface. The amount of detached F20 was so small comparing with the initial intensity of fluorescence (4469.05 ± 432.10).

Cell morphology and adhesion observation on the F20-coated surface

The examination and assessment of the cell adhesion and the morphology were carried out with SEM and CLSM. The cells on the machined surface was round and circular shape with relatively low level of spreading in 6 hours after cell seeding (Fig. 2A). Alternatively, the cell appearance was flat, wide spread and polarized on the F20-coated machined surface (Fig. 2B). Cells on the SLA surface appeared elongated comparing with that on machined surface, (Fig. 2C and 2A) and it is consistent with the previous report. [23] The cytoskeletons were stretched on the F20-coated SLA surface (Fig. 2D).
In 24 hours, the spread of cells seemed similar on both machined and SLA surfaces (Fig. 2E and 2G). The cell appearance of F20-coated surface seemed more elongated and stretched (Fig. 2F and 2H) comparing with that of 12 hours (Fig. 2B and 2D).

11

SEM observation in 6 hours showed more round and less spread morphology (Fig. 2A and 2B) and CLSM observation in 12 hours showed more flat and more stretched and spread morphology (Fig. 3A and 3B).

Compared with the SLA surface, on machined surface cells seemed apparently attached firmly and more stretched. Cells on F20-coated surface seemed elongated and with irregular and stretched (Fig. 3B and 3D) comparing with non F20-coated surface (Fig. 3A and 3C) and that was more prominent on SLA surface.

In 24 hours after cell seeding, cells were remarkably increased in number (Fig. 3E and 3H) comparing with at 6 hours (Fig. 3A and 3D), that was more obvious on machined surface (Fig. 3E and 3F) than on SLA surface (Fig. 3G and 3H). It was consistent with the previous report. [1]
Moreover, on machined surface cells seemed significantly more spread and stretched (Fig. 3E and 3F) than on SLA surface (Fig. 3G and 3H).

Cell migration with F20

The F20 on ST2 cell was examined in an in vitro model, treating 30 µg/ml MMC to arrest cell proliferation. Representative photographs of a F20 concentration of 1µg/ml in each point of time are shown in Fig. 4A.

The cell migration rate was calculated by measurement of the migrated cell area compared with that of control group at 3 hours in 2 mm diameter centrally-located detection zone using an automated image analysis system. In the 3, 6, and 24 h control groups, the mean migration rate were 1 ± 0, 1 ± 0, and 2.3 ± 0.1 respectively. In F20 in a concentration of 1 µm/ml groups, 1.2 ± 0.2, 1.6 ± 0.2, and 3.5 ± 0.3 respectively. There was a significant difference among control group and test group in 6 and 24 h ($p < 0.05$) (Fig. 4B).

Cell proliferation with F20

Picogreen assay was used to analyze proliferation of cells on the discs (Fig. 5A). Cells were seeded and cultured on the discs and harvested in 1, 3, and 5 days.

The proliferation of cells was considerably increased on the machined surface than the SLA surface, and that on F20-coated surfaces showed significant effect on the cell proliferation. The proliferation pattern was analyzed in the CLSM and the result is indicated in Fig. 3.

Osteoblast differentiation with F20

To observe cell differentiation, ST2 cells were cultivated in 1, 4, and 7 days. Quantitative real-time PCR was performed on the well-known bone marker gene ALP (Fig. 5B). The expression of ALP showed significantly improved results on the SLA surface, comparing with that on the machined surface in non F20-treated condition. It is considered from the excellent osteogenic potential of SLA surface itself. [24]

But it was interesting that osteogenic potential level was very similar to that of SLA surface when machined surface was coated with F20.

For the further understanding of the osteogenic potential of F20, ALP activity was tested in 11 days. (Fig. 5C) From ALP activity assay, similar pattern with the expression ALP mRNA was observed. (Fig 5B) ALP activity reached the peak in 8 days.

Erk activation with F20 on Ti surfaces

The increase in the phospho-Erk1/2 (p-Erk) activation in the PDL cells with oligopeptides of PHSRN and RGD was observed to promote the cell attachment in previous report. [17] The stimulation of the Erk pathway by

bone morphogenetic protein-2 (BMP-2) with bone inducing cytokine was also observed. [25] From the base of those findings, p-Erk was treated with F20 in ST2 cells, and observed at 10, 15, and 30 minutes intervals. With F20 treatment, Erk phosphorylation was induced within 10 minutes and it was observed only for a short time (Fig. 6A).

  To confirm that F20-induced osteoblast differentiation is from Erk pathway activation U0126 was used. U0126 is a MEK 1/2 inhibitor and MEK 1/2 is a known as one of Erk upstream kinase. Cells were cultivated to 90% confluency and treated with U0126 of 40 µM and then cultured in solution with F20 (1ng/ml) for 5 days. From ALP staining observation, the interruption against F20-induced ALP activity increase was verified (Fig. 6B). In addition, the influence of U0126 was shown with the quantitative real-time PCR and the suppression of ALP mRNA was observed (Fig. 6C).

From both observations of ALP staining and qPCR, it can be found that the suppression against the expression of ALP with U0126 was not completely inhibited (Fig. 6B and 6C).

IV. DISCUSSION

  Crucially, the most important part for the successful dental implant treatment is to secure the interface between bone and Ti surface. [26] In order to improve these interface circumstances, the previous our researches have replicated the focus on examining the various biomaterials and on characterization of the molecular mechanisms related to cell adhesion, proliferation and differentiation. [20, 23] In this experiment, Ti discs and the F20 were formulated together via an adsorption procedure. Remarkably, the absorption pattern varied with the roughness of the surface (Fig. 1). On the machined surface, F20 was coated in a homogeneous layer. Whereas, F20 coating on SLA surface was signified as the heterogeneous which meant there is a positive relationship between the surface characteristics such as wettability and surface free energy (SFE) and the protein attachment. [27, 28] Wettability and SFE also influenced osseointegration. [29] Conclusively, the peptide adsorption is dependent of the influence of wettability and SFE.

  Different binding affinities are closely associated with the topographical features of SLA surfaces such as the concavity, pit, convexity, and peak. [30] Previous studies reported the negatively charged, polar hydroxyl groups were concentrated on the concavity of SLA surfaces much more than on the convexity. [31] In contrast, binding of F20 on SLA surface was noticeably increased with convex topography comparing with concave topography (Fig. 1B). The increase of F20 coating at peaks of SLA surface can be concluded due to the air pocket (or bubble) formation in the concave pit and it is caused by surface wetting inhibition.

  Additionally, certain amount of F20 which once attached on both kinds of surface was observed to detach and the levels of detachment were slightly

higher on the machined surface. However, the amount or level of this detachment was not significant comparing with the amount of attachment sustained and detached F20 would stay close from the surface of implant. Possibly it may influence on the nearby cell structures to accelerate cell proliferation or differentiation or both.

Comparing with this study, some previous studies reported the consistent results that the cultured cells had shown the increase in differentiation and the decrease in proliferation and it was more prominent on rough surfaces of implant than machined surfaces. [27, 32, 33] Even though the early stage of F20 absorption on smooth surface was highly unstable, the cell adhesion and proliferation was highly influenced. Contrastingly the effect of F20 on rough surface was not remarkable (Figs. 2, 3, and 5A). Furthermore, the machined surfaces showed superior result in binding of F20 in pattern of homogenous laying (Fig. 1B, a). The effect on cellular activity such as adhesion and proliferation of F20 seemed lesser than the effect derived from the surface topography.

The result of this study showed a significant increase in ST2 cell migration rate in F20 at each point in time except the early stage. Previous studies have been reported the consistent results that different cell types such as periodontal ligament fibroblast or MC3T3-E1 cell in wound healing model. [34]

The assessment of osteoblast differentiation was done by the real-time PCR (Fig. 5B) and ALP assay analyses (fig. 5C). It was shown the F20 comprised an exceptional biomolecule suitable for use in surface modification. This was proven by the effects on osteogenesis of cells which cultivation carried out on the machined surface in comparison of the SLA surface, as observed by cell adhesion, proliferation, and differentiation.

For osteoblast differentiation, BMP-2 is a mandatory growth factor [35]. In addition to activate the SMAD pathway, BMP-2 influence the activation of

intracellular signaling molecules in non-SMAD pathway, for example, Erk, mitogen-activated protein kinase (MAPK), c-Jun N-terminal kinases (JNKs), phosphatidylinositol 3-kinase (PI3K), and protein kinases C and D (PKC and PKD). [25]

Various kinase inhibitors were utilized in order to determine which signaling pathway involved F20-induced osteogenesis in ST2 cells (data not shown). One particular pathway from the tests tried, the Erk pathway demonstrated a highly positive relationship with ST2 cells with F20 treatment. (Fig. 6A) To confirm the hypothesis that the F20 stimulated osteogenesis through Erk pathway, U0126 was applied to block the Erk signaling pathway as an inhibitor. Even though the amount was diminished, the osteogenesis still was observed from the result of ALP staining (Fig, 6B) and real-time PCR (Fig. 6C) analyses and not completely blocked.

Under these results, the existence of the alternative compensating signaling pathway besides the Erk pathway can be assumed. Within the limitation of this study focused on Erk pathway, the data was not useful enough to discuss other F20 induced cell response that was promoted with F20 application, such as cell adhesion, migration and proliferation. The clinical approach with F20 adsorption on Ti surface can be considered and the next step further study related with the underlying mechanism of osteoblast differentiation and transcription factors should be investigated.

In conclusion, an FN-derived recombinant RGD-containing oligopeptide F20 applied on Ti surface promoted cell adhesion, migration, proliferation and differentiation to osteoblast. In addition, F20 was observed to stimulate the Erk signaling pathway. In terms of the approach of surface modification, F20 can be considered as a choice of bioactive molecules that promote cell response related with the osteogenesis on Ti implant surface.

V. REFERENCES

1. Anselme K. Osteoblast adhesion on biomaterials. Biomaterials 2000; 21(7): 667-81.

2. Bowers KT, Keller JC, Randolph BA, Wick DG, Michaels CM. Optimization of surface micromorphology for enhanced osteoblast responses in vitro. Int J Oral Maxillofac Implants 1992; 7(3): 302-10.

3. Stanford CM. Surface modifications of dental implants. Aust Dent J 2008; 53 Suppl 1(S26-33).

4. Esposito M, Coulthard P, Thomsen P, Worthington HV. The role of implant surface modifications, shape and material on the success of osseointegrated dental implants. A Cochrane systematic review. Eur J Prosthodont Restor Dent 2005; 13(1): 15-31.

5. Grinnell F, Fibronection and wound healing. J Cell Biochem 1984; 26: 107-16.

6. Johansson S, Svineng G, *et al.* Fibronectin-Integrin interactions. Frontiers in Bioscience 2 1997:126-46.

7. Hood JD, Cheresh DA. Role of integrins in cell invasion and migration. Nat Rev Cancer 2002; 2(2): 91-100.

8. van der Flier A, Sonnenberg A. Function and interactions of integrins. Cell Tissue Res 2001; 305(3): 285-98.

9. Moursi AM, Globus RK, Damsky CH. Interactions between integrin receptors and fibronectin are required for calvarial osteoblast differentiation in vitro. Journal of Cell Science 1997; 110: 2187-96.

10. Puleo DA, Bizios R. Mechanisms of fibronectin-mediated attachment of osteoblasts to substrates in vitro. Bone Miner 1992; 18: 215-26.

11. Obara M. Molecular mechanisms for cell adhesion mediated by fibronectin molecules. Seikagaku 1989; 61: 1462-66.

12. Aota S, Nomizu M, Yamada KM. The short amino acid sequence Pro-His-Ser-Arg-Asn in human fibronectin enhances cell-adhesive function. J Biol Chem 1994; 269: 24756-61.

13. Pankov R, Yamada KM. Fibronectin at a glance. J Cell Sci 2002; 115(20): 3861-3.

14. Nordahl J, Mengarelli-Widholm S, Hultenby K, Reinholt FP. Ultrastructural immunolocalization of fibronectin in epiphyseal and metaphyseal bone of young rats. Calcif Tissue Int 1995; 57(6): 442-9.

15. Kim TI, Lee G, Jang JH, Chung CP, Ku Y. Influence of RGD-containing oligopeptide-coated surface on bone formation in vitro and in vivo. Biotechnol Lett 2007; 29(3): 359-63.

16. Cutler SM, Garcia AJ. Engineering cell adhesive surfaces that direct integrin alpha5beta1 binding using a recombinant fragment of fibronectin. Biomaterials 2003; 24(10): 1759-70.

17. Kim TI, Jang JH, Lee YM, *et al.* Biomimetic approach on human periodontal ligament cells using synthetic oligopeptides. J Periodontol 2004; 75(7): 925-32.

18. Kim YJ, Park YJ, Lee YM, Rhyu IC, Ku Y. The biological effects of fibrin-binding synthetic oligopeptides derived from fibronectin on osteoblast-like cells. J Periodontal Implant Sci 2012; 42(4): 113-8.

19. Lee JA, Ku Y, Rhyu IC, Chung CP, Park YJ. Effects of fibrin-binding oligopeptide on osteopromotion in rabbit calvarial defects. J Periodontal Implant Sci 2010; 40(5): 211-9.

20. Kim TI, Jang JH, Kim HW, Knowles JC, Ku Y. Biomimetic approach to dental implants. Curr Pharm Des 2008; 14(22): 2201-11.

21. Cho YD, Yoon WJ, Kim WJ, *et al.* Epigenetic modifications and canonical Wingless/int-1 Class (WNT) signaling enable trans-differentiation of nonosteogenic cells into osteoblasts. J Biol Chem 2014; 289(29): 20120-8.

22. Cho YD, Hong JS, Ryoo HM*, et al.* Osteogenic responses to zirconia with hydroxyapatite coating by aerosol deposition. J Dent Res 2015; 94(3): 491-99.

23. Feller L, Jadwat Y, Khammissa RA*, et al.* Cellular responses evoked by different surface characteristics of intraosseous titanium implants. Biomed Res Int 2015; 2015: 171945.

24. Orsini G, Assenza B, Scarano A, Piattelli M, Piattelli A. Surface analysis of machined versus sandblasted and acid-etched titanium implants. Int J Oral Maxillofac Implants 2000; 15(6): 779-84.

25. Jun JH, Yoon WJ, Seo SB*, et al.* BMP2-activated Erk/MAP kinase stabilizes Runx2 by increasing p300 levels and histone acetyltransferase activity. J Biol Chem 2010; 285(47): 36410-19.

26. Schwartz Z, Kieswetter K, Dean DD, Boyan BD. Underlying mechanisms at the bone-surface interface during regeneration. J Periodontal Res 1997; 32(1-2): 166-71.

27. Ponsonnet L, Reybier K, Jaffrezic N*, et al.* Relationship between surface properties (roughness, wettability) of titanium and titanium alloys and cell behaviour. Materials Science & Engineering C-Biomimetic and Supramolecular Systems 2003; 23(4): 551-60.

28. Boyan BD, Lohmann CH, Dean DD*, et al.* Mechanisms involved in osteoblast response to implant surface morphology. Annual Review of Materials Research 2001; 31: 357-71.

29. Cochran DL, Buser D, ten Bruggenkate CM*, et al.* The use of reduced healing times on ITI (R) implants with a sandblasted and acid-etched (SLA) surface: Early results from clinical trials on ITI (R) SLA implants. Clin Oral Implants Res 2002; 13(2): 144-53.

30. Pegueroles M, Aparicio C, Bosio M*, et al.* Spatial organization of osteoblast fibronectin matrix on titanium surfaces: effects of roughness, chemical heterogeneity and surface energy. Acta Biomater 2010; 6(1): 291-301.

31. Wang XX, Hayakawa S, Tsuru K, Osaka A. A comparative study of in vitro apatite deposition on heat-, H2O2-, and NaOH-treated titanium surfaces. J Biomed Mater Res 2001; 54(2): 172-78.

32. Schwartz Z, Martin JY, Dean DD, *et al.* Effect of titanium surface roughness on chondrocyte proliferation, matrix production, and differentiation depends on the state of cell maturation. J Biomed Mater Res 1996; 30(2): 145-155.

33. Anselme K, Bigerelle M, Noel B, *et al.* Qualitative and quantitative study of human osteoblast adhesion on materials with various surface roughnesses. J Biomed Mater Res 2000; 49(2): 155-66.

34. Park BS, Heo SJ, Kim CS, Oh JE, Kim JM, Lee G, *et al*. Effect of adhesion molecules on the behavior of osteoblast-like cells and normal human fibroblasts on different titanium surfaces. J Biomed Mater Res 2005; 74: 640-51.

35. Chen D, Zhao M, Mundy GR. Bone morphogenetic proteins. Growth Factors 2004; 22(4): 233-241.
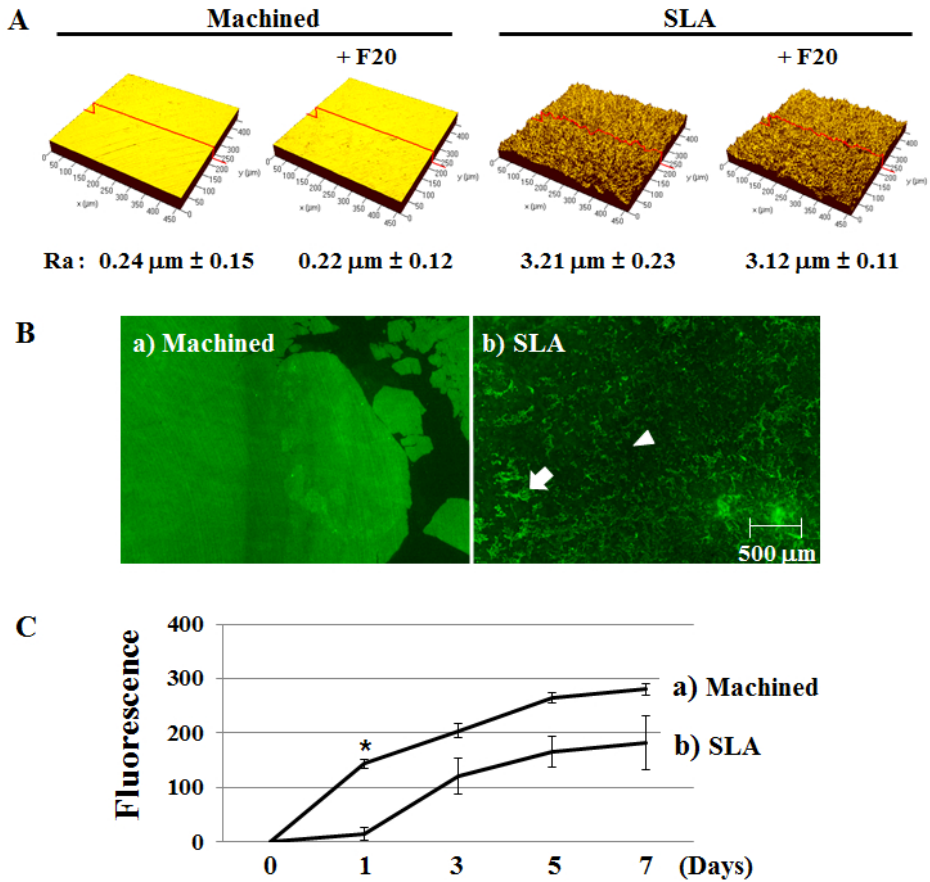
Figure legends

Fig. 1. A. Confocal laser scanning microscopy (CLSM) image showing the roughness (R_a) of the Ti surfaces. B. Distribution of absorbed fluorescein isothiocyanate (FITC)-labeled F20 on Ti surfaces with different levels of surface roughness, as determined by fluorescence microscopy. a) Machined Ti surface; b) sand-blasted, large grit, acid-etched (SLA) Ti surface. Arrow indicates a convex peak in the surface topography with bright fluorescence. Arrowhead indicates a concave pit with low fluorescence. Original magnification is 40×; bar = 500 μm. C. Fluorescence intensity was measured

in the culture media over 7 d. Samples were normalized by subtracting the day 0 basal value from all other measurements. a) Machined Ti surface; b) SLA Ti surface. *$p < 0.05$ against SLA Ti.
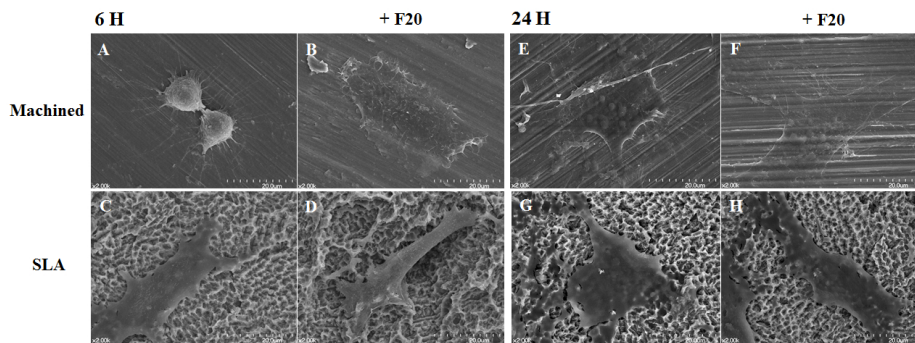
Fig. 2. Scanning electron microscopy (SEM) images showing ST2 cell adhesion and morphology on distinct titanium disc surfaces. A–D. At 6 h after cell seeding; E–H. At 24 h after cell seeding. A and E. Machined Ti; B and F. F20-coated machined Ti; C and G. sand-blasted, large grit, acid-etched (SLA) Ti; D and H. F20-coated SLA Ti. Images were obtained at 2,000× magnification; bar = 20 μm.
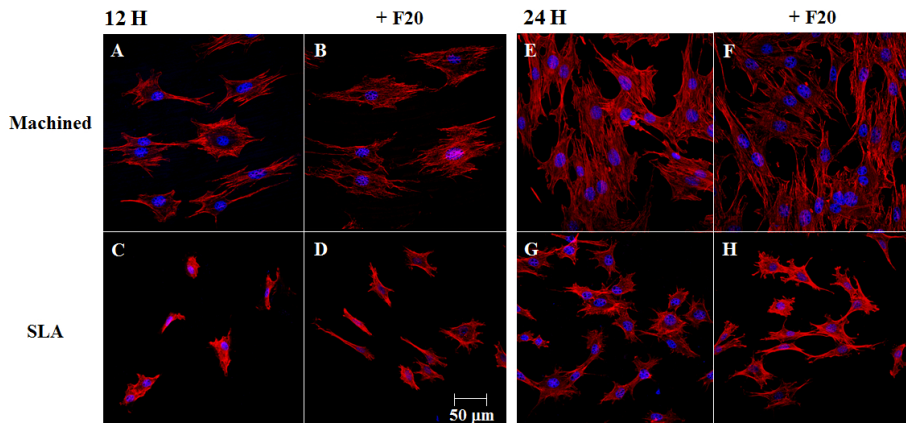
Fig. 3. Confocal images of ST2 cells at 12 and 24 h after seeding on distinct Ti disc surfaces. A and E. Machined Ti; B and F. F20-coated machined Ti; C and G. sand-blasted, large grit, acid-etched (SLA) Ti; D and H. F20-coated SLA Ti. Original magnification is 300×; bar = 50 μm.
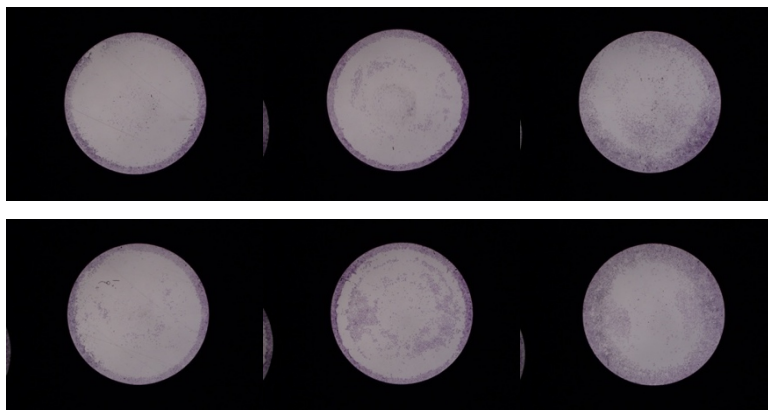

Fig. 4. A. Light microscopic images fixed with 10% NBF and stained with 0.25% (w/v) toluidine blue at the 2 mm detection zone of the cell migration

assay kit with a detection mask at 3, 6, 24 h. Magnification x40. Control and F20 (1 ng/ml). The migration of cells from the initial position of stopper margin was observed and the degree of spread was different with time and media. The migration rate was calculated by the area of cell spread which is moved centrally compared with the area of cell spread which outside the stopper position in the 2 mm detection zone.
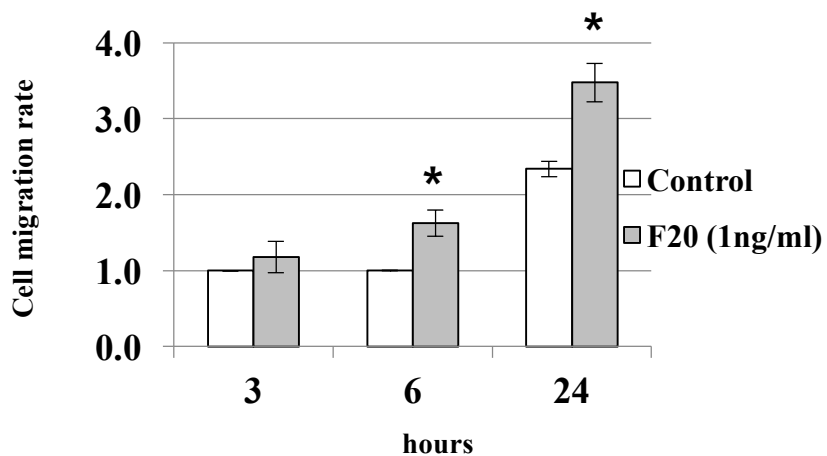
B. Control and F20 on migration rate in the detection zone at each point in time 3, 6, 24 hours (*$p < 0.05$).
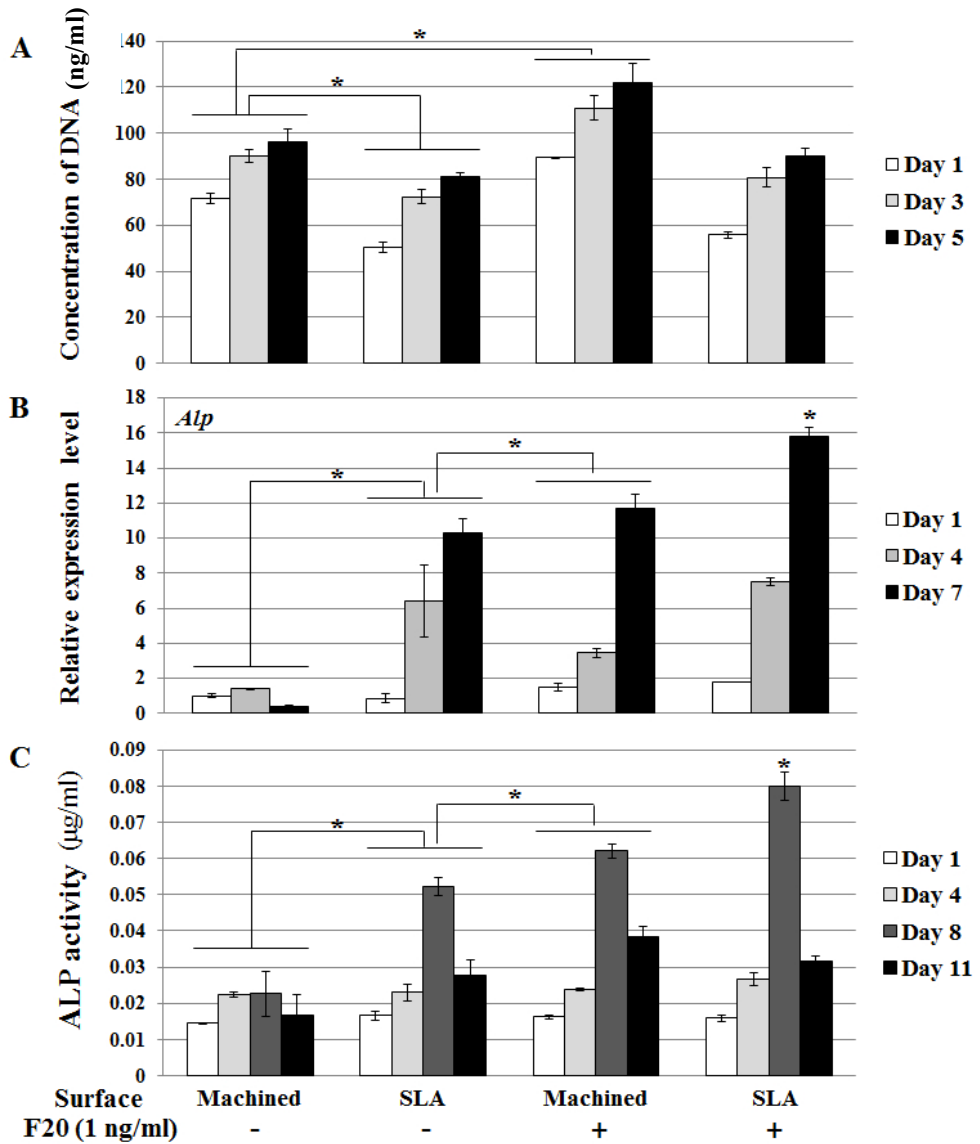
Fig. 5. A. Picogreen assay-based analysis of proliferation of ST2 cells on distinct Ti discs after 1, 3, and 5 days of culturing. B. Real-time PCR analysis of alkaline phosphatase (*ALP*) mRNA expression in ST2 cells on the Ti discs after 1, 4, and 7 days of culturing. C. ALP activity assay analysis. Cells were

seeded on Ti discs and cultured for 11 days. ALP activity was measured as indicated in the Materials and Methods section. The data are expressed as means ± standard deviations (SD) of the results from three independent experiments (*$p < 0.05$).
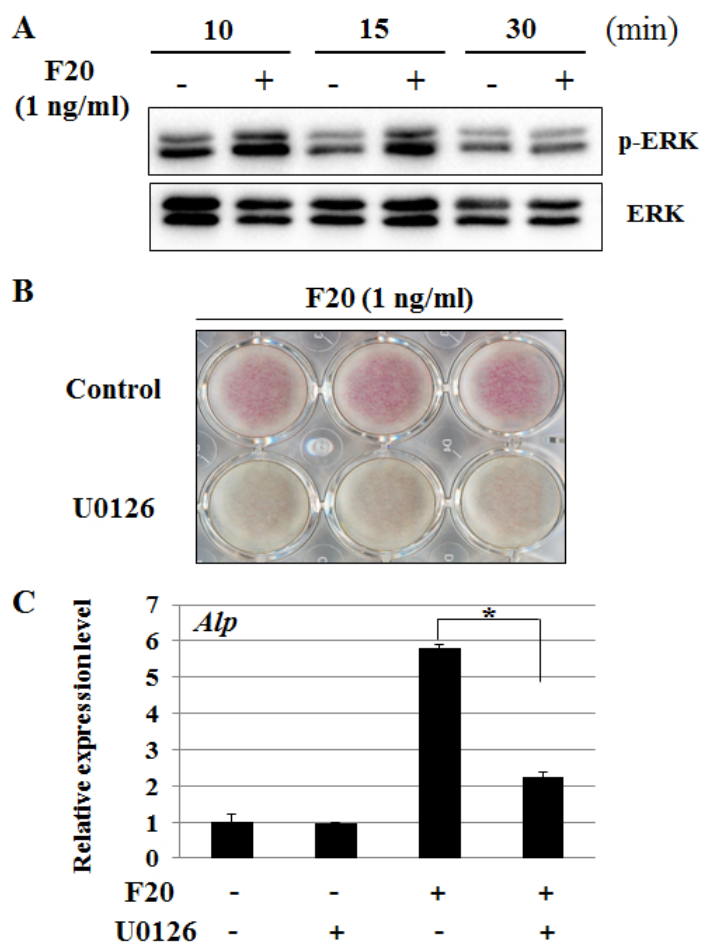

Fig. 6. A. Detection of extracellular signal-regulated kinase (Erk)1/2 and phospho-Erk1/2 levels in ST2 cells treated with F20 (1 ng/ml) at the indicated

times by immunoblot analysis. B and C. Alkaline phosphatase (ALP) staining and real-time PCR analysis of cells treated with the Erk inhibitor U0126, respectively. U0126 suppressed F20-induced (B) ALP activity and (C) *Alp* mRNA expression. The data are expressed as means ± standard deviations (SD) of the results from three independent experiments (*$p < 0.05$).

국문초록

합성펩타이드로 표면처리된 티타늄이 골형성에 미치는 영향

김 성 준

서울대학교 대학원 치의학과 치주과학 전공

(지도교수 구 영)

세포 및 동물실험을 통한 선행연구에서 파이브로넥틴(Fibronectin, FN) 유래 올리고펩타이드(F20) 가 조골세포의 분화 및 골형성을 증진시키는 것을 확인한 바 있다. 이 연구의 목적은 치과용 임플란트 재료로 널리 사용되고 있는 티타늄의 표면에 F20 을 접착시킨 표면개질이 조골세포의 분화에 미치는 영향과 그 기전을 알아보는 것이다.

기계절삭 표면(machined) 및 산부식 처리(Sandblasted and acid-etched, SLA)된 티타늄 디스크를 제작한 후, 공초점 레이저 현미경(Confocal Laser Scanning Microscopy, CLSM) 관찰을 통해 티타늄의 표면 특성 분석을 하였다.

F20 의 접착수준을 확인하기 위해 형광(Fluorescein isothiocyanate, FITC)을 표지한 F20 을 사용하였으며, 형광현미경을 이용하여 접착 패턴을 분석하였다. 또한, 조골세포로 분화하는 것으로 알려진 골수기질 유래세포인 ST2 세포를 티타늄 디스크 위에 배양하고 주사전자현미경(SEM)과 CLSM 을 이용하여 초기 세포 부착 수준을 평가하였다. 세포이동분석(Cell migration assay)를 통해 F20 의 세포

이동에의 영향을 관찰하고, 피코그린(Picogreen) 분석법을 이용하여 세포 배양 1, 3, 5 일 후의 세포의 증식 정도를 측정하였다. 또한 real time PCR, ALP 활성분석 및 ALP 염색을 이용하여 조골세포로의 분화 정도를 평가하였다.

디스크 표면의 특성에 따라 F20 은 기계절삭 표면에서는 균일한 층판 모양으로, SLA 표면에서는 점상 형태(dotted pattern)로 접착된 양상을 보였으며, 디스크에 배양한 세포들은 SLA 보다는 기계절삭 표면에서 초기 부착이 잘 일어났다. F20 처리된 군에서는 비처리군에 비해 전체적으로 신장된 형태의 세포가 관찰되었으며, 세포 증식 또한 기계절삭 표면에서 높게 나타났을 뿐 아니라, F20 으로 처리하였을 때 증가하였다. 세포의 이동도 F20 처리후 대조군에 비해 향상된 결과를 보였으며 조골세포의 분화는 SLA 표면에서 잘 일어났으며, F20 은 분화를 촉진시키는 역할을 하였는데, 이는 Erk/MAPK 신호전달을 통해 이루어짐을 확인 할 수 있었다.

본 연구의 결과, 티타늄 디스크 표면의 F20 접착 처리는 조골세포의 분화를 촉진시킴을 알 수 있었으며, 이는 티타늄 표면에 파이브로넥틴유래 올리고펩타이드(F20)를 이용한 표면개질이 골형성능을 높일 수 있음을 보여주었다. 향후, 사용된 펩타이드를 티타늄 표면에 더 안정적으로 적용시킬 수 있는 전략에 대한 연구개발이 필요할 것으로 생각된다.

주요어: 파이브로넥틴, 올리고펩타이드, 치과용 임플란트, 표면개질, 조골세포 분화

학번: 2005-30736